Characterization of barrier properties for stretch blow moulded polypropylene and PET

Gravelle, A.; DiRaddo, R.; Deschenes, L.; Tung, M. A.

https://doi.org/10.4224/23003017

National Research Council Canada
Industrial Materials Institute
75 de Mortagne Boulevard
Boucherville, Québec
J4B 6Y4

Conseil national de recherches Canada
Institut des matériaux industriels
75, boulevard de Mortagne
Boucherville, Québec
J4B 6Y4

NRC · CNRC

Characterization of Barrier Properties for Stretch Blow Moulded Polypropylene and PET

A. Gravelle, R. DiRaddo, L. Deschênes and M.A. Tung

IMI / Process Modelling and Optimization

December 1996

Canada

OUTLINE

Introduction

The prediction of the barrier performance of a polymer container moulded at given operating conditions would be a great asset to any food packaging manufacturer. In order to properly predict the container's barrier performance, one needs good characterization data relating permeability to the level of orientation and crystallinity. This work attempts to derive an adequate model to fit and extrapolate findings to predict the permeability coefficient as a function of two important factors affecting the permeability of polymer membranes to gases, crystallinity and orientation. The semi-empirical model makes use of experimental data obtained from containers moulded on an one-stage Injection Stretch Blow Moulding (ISBM) machine and tested on a Differential Scanning Calorimeter and a Mocon Oxtran 10/50 permeability apparatus.

During the design and fabrication of polymer packaging for food use, the permeability of the container to gases is of primordial importance since these may have detrimental effects on the product. Generic data and estimation models for the permeability of polymers exist in the literature which are adequate for polymer films, but more often than not prove to lack precision and accuracy for moulded containers. This is due to the non-uniform thickness distribution of the packaging wall, accompanied by variations in crystallinity and orientation, causing the aforementioned methods to fail. Therefore, in this study, various models predicting permeability as a function of crystallinity and orientation are compared and fitted to experimental data obtained from the side panel of polypropylene beverage bottles.

Once a model is found to represent well the permeability of the polymer, it can be applied to the discretised surface of a whole container which will increase the accuracy of results by taking into account the variations in thickness, crystallinity, and orientation. This becomes greatly beneficial when designing a container intended for food use since adequate shelf life is primordial. The container's thickness can then be optimised to provide an adequate gas barrier without using excess material. It also facilitates the task of identifying potential problem areas where high permeation may occur. Such a method can finally help in the optimisation of the processing stage, since the model relates permeability to the polymer's final morphology, which in turn is controlled by the processing conditions. The objectives of this work are to:

- Characterise the barrier properties of blow moulded polypropylene and PET in order to predict its permeability to oxygen as a function of crystallinity content and degree of orientation.
- Identify a good model to approximate the results of the characterization.

Background

The characterization of the transport properties of polymers and estimation of the resulting transfer rates based on it have widely been investigated. Progress has been made in the field since Fick (1) introduced the first equations for diffusion.

It has been generally accepted that the two most important factors affecting the permeability of a polymeric membrane to permanent gases are its crystallinity and orientation. These have consequently been the subject of several research papers.

Orientation

The effect of orientation was investigated by Wang and Porter (2) who examined the solubility and diffusivity of CO_2 into uniaxially drawn Polystyrene and High Density Polyethylene. They concluded that the effect of drawing has an impact on diffusivity, while maintaining a constant solubility. They also observed that polyethylene, unlike polystyrene, experienced an increase in crystallinity upon drawing, causing the permeability to decrease logarithmically with crystallinity and orientation.

Webb et al. (3) also looked at the effect of one-way drawing on permeability. They tested the barrier properties of polyethylene homopolymers and copolymers exposed to He, CO_2, O_2, and N_2. A decrease in diffusivity with an increase in drawing was also noticed in their study. The solubility was slightly affected. The materials were characterised by density, birefringence and modulus, DSC, and wide angle x-ray spectroscopy. Little difference was noticed between the behaviour of the homopolymer and the copolymer.

The impact of draw ratio on the permeability, diffusivity and solubility of N_2, CO_2, and CH_4, through rolltruded isotactic Polypropylene was studied by Ciora and Magill (4). They determined that under rolltrusion processing conditions, the draw ratio had little effect on the transport coefficients and therefore concluded that the processing conditions have a serious impact on the final transport properties of the material.

The effect of the orientation of PET on its transport properties have also been examined. Swaroop (5) looked at the transport of O_2 and H_2O through oriented flat sheets as well as through blow molded bottles. He noticed that permeability decreased on either side of an abrupt drop at moderate orientation. Permeability to O_2 increased with an increase in the material's intrinsic viscosity. The permeability to H_2O displayed the opposite behavior.

Crystallinity

The effect of crystallinity on the polymer's permeability can be summarised by stating that crystallites formed within the polymer are essentially impermeable, high density structures. This forces the diffusing molecules to weave between them to cross the membrane. The path followed by the molecule is commonly call the tortuous path. Since it is known to have a drastic effect on the final permeability of the polymer, the crystal formation and growth behaviour is of utmost importance. Many have studied this process. Magill (6) reviewed the rate of crystallisation of polymers. Patel and Spruiell (7) surveyed available methods to deal with polymer crystallisation for process modelling. Aubert et al. (8) applied existing methodology to blow moulding applications.

Weurth (9) conducted an in depth study of gas permeation through polypropylene. He analysed the diffusivity and solubility of He, A, and CH_4 independently. He determined that diffusivity reaches a minimum at approximately 60% crystallinity content and then increases with crystallinity. His work was reviewed by Vieth (10).

Processing Conditions

Several publications pertaining to permeability of polymers put emphasis on the effect of processing conditions on the polymer's final morphology. The effect of annealing temperature and molecular weight of biaxially oriented Polyethylene terephthalate beverage bottles on the resulting crystallinity and permeability to O_2 was studied by Perkins (11). Annealing temperature was found to affect permeability more directly than absolute crystallinity. A similar research was conducted by Kim (12). He analysed the effect of the preheat time of PET preforms on the transmission rate of O_2 from the side panel of 2 litre beverage bottles.

Free blowing preforms has proved to be a useful technique in the past for several reasons. Leigner (13) examined the effect of preform design by free blowing them at different blow temperatures and pressures. The effect of using resins of different intrinsic viscosities which represent differing molecular weights was also examined. Venkateswaran and Jabarin (14) studied the effect of moisture and physical aging on the free blow characteristics of PET preforms. They determined that both axial and hoop stretch ratios increase with moisture content in the preform. Aging effects were encountered after 2 weeks for both the wet and dry preforms but these were erased upon reheating of the preform.

Prediction Methods

Several models used to predict the permeability of polymers have been derived based on different concepts. The two-phase method, as presented by Comyn (15)

and Ciora & Magill (4) is very simple. It is based on the existence of two phases within the material consisting of a crystalline phase, considered to be impermeable and the amorphous phase, in which the molecules are free to diffuse. Gohil (16) successfully attempted to use the total phenyl ring orientation factor (PROF) of PET to predict the permeability of biaxially oriented films prepared under different processing conditions.

A model which has gained popularity was devised by Salame (17). It attempts to predict permeability based on the repeating monomer's composition and the diffusing gas at hand. Along with a review of some permeability prediction methods for various polymers, Bicerano (18) presents the "Newcor" method, a variation of Salame's "Permacor" method. The "Newcor" enables the prediction of permeability without having to rely on the availability of group contributions. It can therefore be applied to a wider range of polymers. This allows the method to be applied to chemical structures possessing segmental groups not covered by the "Permacor" method. Jia and Xu (19) have introduced a method similar to the "Newcor", based on the ratio of molar free volume to molar cohesive energy.

The prediction of the permeability of polymer blends such as PET/EVOH and PEN/EVOH is investigated in work performed by Kit et al. (20). The model of Fricke was used to adequately predict the permeability of the polymers. Also included in the same work is an analysis of the effect of orientation on the final morphology of the blends.

This paper will compare experimental data from polypropylene data to the predictions calculated using two of these methods. The first of which is the two phase method, the most primitive of the aforementioned group but the simplest to apply. The second method is the "Permacor", a more recent and well-founded equation. It has been selected over the "Newcor" because of its ease of application since "Permacor" values for the polymer investigated were available. The PET results displayed very limited change in properties within the range of processing conditions tested and so no attempt to derive a representative model for it was made at this time. Further details on these materials follow in the report.

Methodology

In single layer polymer films, it is usually accepted to assume that the transfer rate of permanent gases can be estimated with the use of Fick's law of diffusion,

$$J = -D \times \partial c / \partial x \qquad (1)$$

Where:

J = Diffusive flux of the penetrant
D = Diffusivity coefficient
c = Penetrant concentration
x = Membrane thickness

The diffusive flux is the amount of gas flowing through a membrane of unit area normal to the surface of thickness x. At low pressures (<1 atm), the sorption of

permanent gases into the membrane obeys Henry's law (21),

$$c = S \times p \qquad (2)$$

Where:

S = Solubility coefficient
p = partial pressure of diffusing gas

which indicates that the concentration of the penetrant is proportional to the partial pressure of the gas in question. By combining equations (1) and (2), and knowing that the solubility of the product into the membrane and its diffusivity through it yields the permeability,

$$P = S \times D \qquad (3)$$

Where:

P = Permeability coefficient

Equation (1) becomes,

$$J = P \times \frac{(p_1 - p_2)}{l} \qquad (4)$$

Where:

l = thickness of membrane
p_1 ,p_2 = partial pressure of gas on either side of the membrane

It is therefore essential to determine the value of the permeability coefficient P if the transfer flux and consequently the potential shelf-life offered by the container is to be determined.

Published values of the permeability coefficient of polypropylene and polyethylene terephthalate are vastly available (22-24). The problem that arises when using these values is that in most cases, they were obtained from analyses following ASTM and/or BSI methodology on annealed and relatively unoriented test specimens. Normal injection stretch blow moulding conditions produces a polymer that has different crystallinity and orientation combinations which may not correspond with the conditions on the polymer from which the generic data was obtained.

An approach taken in the past to predict the permeability coefficient of a plastic was to consider the polymer as being composed of two phases, an impermeable phase consisting of crystalline structures confined within a permeable amorphous second phase. The permeation process occurs in two steps: the solution of the gas into the membrane, followed by its diffusion through the polymer. This approach was the foundation for the 2 phase model to predict permeability. The solution is expressed through:

$$S = S_{nc} \times \left(\frac{100 - Xc}{100} \right) \tag{5}$$

Where:

S_{nc} = Solubility coefficient of 100% amorphous polymer
Xc = Relative Crystallinity (%)

Equation (5) is the theoretical gas solubility coefficient in polymers as a function of crystalline content. This behaviour has been observed for various systems several times in the past (25-28). The diffusion of gas is represented by:

$$D = D_{nc} \times \left(\frac{100 - Xc}{100} \right)^{b} \tag{6}$$

Where:

D_{nc} = Diffusivity coefficient of 100% amorphous polymer
b = equation parameter dependant on polymer

Equation (6) attempts to predict the diffusivity coefficient of a gas through a polymer as a function of the crystalline content. Some confusion exists with the proper value to use for the exponent, b. It has been published (4) that its value ranges between 1 and 2 for different polymers. Another source (15) states that the exponent ranges between 0.3 for polyethylene, to 1.0 for PET. When the value of the exponent is within 0.3 and 2.0, a decrease in permeability with increasing crystalline content is observed.

Equations (5) and (6) can be substituted into equation (3) to get the predicted permeability coefficient at any relative crystallinity.

$$P = P_{nc}\left(\frac{(100 - Xc)}{100}\right)^{(b+1)} \qquad (7)$$

Where:

P_{nc} = Permeability Coefficient of 100% amorphous polymer
b = equation parameter dependant on polymer

One problem with this model is that it neglects to consider the effect of several factors on permeability other than crystallinity. The permeability of a polymer depends on many structural parameters such as orientation, crystallinity, free volume, polarity, tacticity, cross-linking and grafting, and the presence of additives (29), with the former two recognised as being the major properties affecting permeability.

Salame (17) developed the Permacor method to predict the permeability of polymers to gases. Along with its consideration for crystallinity and orientation, the method takes into account two very fundamental properties of the polymer: cohesive energy density and the amount of free volume. The former is a measure of how tightly the chains are bound to each other, while the latter is the free volume between the chains allowing movement of the gas molecules.

Given the chemical structure of the repeating monomer, a value is attributed to each segmental backbone and side chain groups, resulting in the polymer Permacor (π_a). This value is for a 100% amorphous material. The degree of crystallinity will alter this number by:

$$\pi = \pi_a - 18\ln\left(\frac{(100 - Xc)}{100}\right) \tag{8}$$

Where:

π = Permacor adjusted for crystalline content

After taking into account factors such as the jump step needed for the molecule to diffuse, the diameter of the gas, the volume needed and the polymer forces acting against diffusion, the permeability equation becomes,

$$P = \left(A/\tau_o\right)e^{-s\pi} \tag{9}$$

Where:

A,s = Gas constants for Permacor method

τ_o = Tortuosity caused by orientation of crystallites

The degree of orientation is taken into account by the inclusion of a tortuosity value into the permeability equation. For unoriented polymers, τ_o is equal to 1. For polymers oriented 200 to 300%, τ_o changes with crystallinity following,

$$\tau_o \cong 1.13\Big/\sqrt{\left(\frac{(100 - Xc)}{100}\right)} \tag{10}$$

This approach has been successful with over 60 polymers and can be used with several different gases. In his paper, Salame provides all the necessary Permacor values of segmental groups to facilitate the calculation. The validity of the above equations for injection stretch blow-moulding applications still remains to be examined.

Experimental

Materials

The first material used for analysis was the Pro-fax SR-549M Polypropylene manufactured by Montell North America Inc. It is a copolymer having a density of

0.90g/cm^3 and a melt flow rate of 11dg/min. It offers high clarity, good organoleptic properties for food-contact and is designed for injection moulding and injection stretch blow moulding.

The second resin utilised was Eastman Chemical Company's Kodapak PET 9921 clear copolyester. It has an intrinsic viscosity of 0.80. It is Kodak's resin of choice for carbonated beverages, cosmetics, food, and water.

Sample preparation

A 3-stage injection stretch blow moulding (ISBM) machine (model # SB III-100H-15) was used to blow mould the containers.

Polypropylene

The polymer melt temperature for polypropylene was 215°C during injection into the preform mould which was kept at a temperature of 9.0±1°C for all samples. Primary and secondary injection pressures were maintained at 689.5 kPa and 3447.5 kPa, respectively for both resins. The back pressure was 517.1 kPa. The primary and secondary blow pressures were 1379 kPa and 517.1 kPa, respectively.

The first sample bottles were fabricated with a blow mould present, which constrained the inflating preform and forced it to adopt the dimensions of a 476 ml polypropylene cylindrical beverage bottle. This assured a constant stretch ratio and allowed for an analysis of the effects of various processing conditions on the relative crystallinity of the container's side panel.

The effect of varying the blow mould temperature and the inflation time were examined. The blow mould temperature was varied between 10°C, the minimum temperature that could be reached by the equipment, up to a temperature of 93°C. The holding time within the mould was tested at intervals ranging from 1 to 10 seconds. Longer time intervals allowed the following preform to cool too much to be inflated.

Some preforms were inflated in the absence of the blow mould. Bubbles of different stretch ratios could then be fabricated by varying the blow time. This method has been used in the past with PET to determine the blow characteristics of the preform (30). This procedure provided samples of different crystallinity/stretch ratio combinations.

The blow time for the free-blown containers was varied between 0.1 seconds to 0.7 seconds. Shorter periods did not inflate the preform, while longer time periods

caused the bottle to burst.

The stretch ratio was calculated by taking the geometric mean of the radial and longitudinal stretch ratios of the final bottle over the initial preform at the mid-point of the side panel, 180° from the clamping head code imprint on the bottle's brim. The measured height of the bottles and preforms was taken as the distance from the collar of the bottle to the centre of the bottom of the bottle, since no deformation occurs at the clamped end above the collar.

$$SR_{Radial} = \frac{RADIUS_{Bottle}}{RADIUS_{Preform}} \tag{11}$$

$$SR_{Longitudinal} = \frac{HEIGHT_{Bottle}}{HEIGHT_{Preform}} \tag{12}$$

$$SR_{Mean} = \sqrt{SR_{Radial} \times SR_{Longitudinal}} \tag{13}$$

Finally, unstretched, unblown preforms were collected to serve as samples having a stretch ratio of 1.

Polyethylene Terephthalate

The polymer melt temperature for polyethylene terephthalate was 275°C during injection into the preform mould which was kept at a temperature of 9.0±1°C for the blow moulded samples. The preform mould temperature was varied for the free blow tests performed with the PET. Primary and secondary injection pressures were maintained at 689.5 kPa and 3447.5 kPa, respectively for both resins. The back pressure was 517.1 kPa. The primary and secondary blow pressures were 1723.7 kPa and 517.1 kPa respectively for PET. The material was dried at a temperature of 150°C for a period of 4 hours prior to moulding.

The blow moulded PET bottles were inflated within a 750 ml rectangular beverage bottle mould. This assured a constant stretch ratio and allowed for an analysis of the effects of various processing conditions on the relative crystallinity of the container's side panel.

The effect of varying the blow mould temperature and the inflation time were examined. The blow mould temperature was varied between 10°C, the minimum temperature that could be reached by the equipment, up to a temperature of 50°C. The holding time within the mould was tested at intervals ranging from 2 to 8

seconds.

The blow time for the free-blown containers was varied between 0.15 seconds to 0.55 seconds for PET. Shorter periods did not inflate the preform, while longer time periods caused the bottle to burst due to strain hardening. Stress whitening was also noticeable at blow times above 0.55 seconds. The preform mould temperature for the free blow testing was maintained at 32.2°C which was the highest temperature at which a preform could be formed without any deformation occurring upon removal of the preform from its mould.

Equations (11-13) were used to calculate the stretch ratio for the samples examined. The area tested was taken from the outermost point of the bubble, directly below the head code imprint on the bottle's brim.

Thermal Analysis

Polypropylene

All samples were taken within a 3 cm^2 area where the stretch ratio measurements were taken. A hole punch was used to cut circular samples from the bottles which were then placed in aluminium pans for the analysis. The furnace of both instruments were flushed with nitrogen gas. The sample weights were between 5 and 15 mg. Between 1 and 3 sample disks were needed to meet the weight requirement.

The melting peak of the sample containers were measured on a Perkin-Elmer DSC 7 as well as a Mettler DSC-30. When using the Mettler DSC, the type 16 baseline, recommended for polymers, was selected for analysis. Indium was used to calibrate both instruments. The analysis was conducted at a constant heating rate of 20 °C min^{-1}. The crystallinity of the samples was calculated from:

$$Xc = \frac{\Delta H_f}{\Delta H^*_f} \times 100\% \qquad (14)$$

Where:

Xc = Relative Crystallinity (%)

ΔH_f = enthalpy of sample

ΔH^*_f = enthalpy of 100% crystalline sample

The value of ΔH_f is the area under the melting peak of the analysed sample, representing the latent heat of fusion of the sample. The value for ΔH^*_f was determined experimentally to be 93.57 J/g on the DSC-7 for polypropylene. The

latent heat of a 100% crystalline polypropylene sample on the Dupont DSC was found to be 88.0 J/g through peak integration. The method used to prepare and measure the fully crystalline sample was the same as the one followed by Aubert et al. (7).

Polyethylene Terephthalate

A similar technique used to analyse polypropylene samples was followed to analyse the PET but modifications were required. A heating rate of 10 °C min^{-1} was required in order to increase the precision of the endothermic peak of crystallisation. Because of the crystallisation of PET during the calorimetric heat treatment, this peak must be subtracted from the peak of fusion in order to get the real latent heat of fusion, ΔH_f, which in turn will allow the determination of the sample's original crystalline content. Mehta et al. (31) determined that a value of 140J/g is a good prediction of the heat of fusion of 100% crystalline PET.

Permeability Analysis

Polypropylene

The permeability of the samples to oxygen was tested on a Mocon Oxtran 10/50. The side panels of the moulded bottles were tested with a 100% oxygen, 0% RH environment at the outer surface of the polypropylene membranes. The 10 cm x 10 cm section was taken such that the middle of the surface tested was the mid-point of the side panel, 180° from the clamping head code imprint on the bottle's brim. Nitrogen was used as the carrier gas at the inner surface of all the films.

The samples from the free-blown containers had small radii of curvature and therefore necessitated the use of 5 cm^2 masks in order to be properly installed on the instrument.

Films were left to condition for at least 24 hours on the instrument before Oxygen Transmission Rate (OTR) readings were taken. By monitoring readings, it was determined that steady state had been reached within this period for polypropylene.

The preforms were mounted on a brass plate specially built to flush the inside of the preform with the carrier gas. "Luctite 416" gap filling glue was used to create a hermetic seal between the plate and the preforms. The outside of the preform was exposed to air, reducing the outer partial pressure to 21% of the atmospheric pressure. The OTR reading was also multiplied by the area setting on the data logger (50 cm^2) and divided by its true surface area, which was 84.71 cm^2 .

The permeability coefficient could then be determined by multiplying the OTR by the average thickness of the sample and dividing by the atmospheric pressure. The thickness of the samples was measured with a MAGNAMIKE (model 8000), consisting of a magnetic probe and a 3.2 mm steel target.

Polyethylene Terephthalate

The same test procedure followed for the polypropylene samples was used for PET aside from a few modifications which are as follows. The tests performed on the PET samples were conducted under "real-life" conditions, with 100% RH at the inner surface of the film while the external surface was exposed to a 45% RH environment.

The samples to be tested were taken from the wide side panel located below the head code imprint of the rectangular PET bottles The samples were left on the apparatus for a minimum period of 72 hours, the time required to assure the attainment of steady state.

The OTR reading was also multiplied by the area setting on the data logger (50 cm^2) and divided by its true surface area, 102.06 cm^2 .

Units

Over thirty different units for P appear in literature. The ones chosen for this study, are in accordance with SI system units, as adopted in Polymer Handbook (23).

$$UNITS = \frac{cc(STP) \times cm}{cm^2 \times s \times Pa}$$

Results and Discussion

Blow Moulded Containers-Crystallinity and Stretch Ratio

Polypropylene

The temperature of the blow mould and the contact time between the blow mould and the inflated bottle had a noticeable effect on the final degree of crystallinity of the bottle. As depicted in figure (1), crystallinity slightly declined with increasing exposure time at low mould temperatures. At a temperature of 93 degrees Celsius, an upward trend was observed.

This change in behaviour is suspected to be caused by a variation in cooling patterns. The heat transfer rate is much higher when the bottle is in contact with the mould than when exposed to ambient air. The time the bottle spends in the mould will therefore have an impact on the degree of crystal growth. The effectiveness of the heat transfer also depends on the temperature gradient present in the system. For a given time interval, low mould temperatures produced polymers having lower crystallinity than at high mould temperatures. At 93° Celsius, the temperature gradient between the mould and the bottle becomes small, to the point where the mould has somewhat of an annealing effect on the bottle, which would explain the increase in relative crystallinity with time spent in the mould.

Polyethylene Terephthalate

The DSC results from the analysis of the side panels of blow moulded bottles, presented in table 1, revealed that residence time of the bottle within the blow mould had no noticeable effect on crystallinity within the range of conditions tested.

The small increase in crystallinity with increasing mould temperature can be attributed to a decrease in temperature gradient at the polymer/mould interface which would lower the cooling rate of the bottle. This in turn would allow the bottle to remain in the crystal growth temperature range for a slightly longer period of time, which would account for the ~0.5% increase in crystallinity. This worth of this hypothesis is limited due to the lack of precision that the peak integration analysis technique offers.

Table 1: Relative Crystallinity of Blow Moulded Bottles as a Function of Blow Mould Temperature and Bottle Residence Time within Blow Mould

	Blow Mould Temperature (°C)			
Residence Time of Bottle within Blow Mould (s)	**10**	**16**	**35**	**50**
2	30.27%	-----	-----	30.59%
4	-----	30.38%	-----	31.02%
6	30.31%	-----	30.34%	-----
8	30.48%	-----	-----	30.68%

All the DSC plots for the above samples had no crystallisation peak. This suggests that the bottles have reached their maximum crystallinity level of ~30% since further crystallisation did not occur upon heating in the DSC furnace.

The crystallinity of an undrawn preform allowed to cool at room temperature was also tested with the DSC. The results revealed a crystallinity of 8.7%. A crystallisation peak was present on the DSC plots, indicating that complete crystallisation was not achieved. From these results, it becomes apparent that the increase in crystallisation in the blow moulded samples must have been stress-induced upon stretching and blowing of the preform. Otherwise, the preform, which had a slower cooling rate than the other samples and therefore remained longer within the crystallisation temperature range, would have certainly surpassed the bottles' crystalline content, or at least reached its maximum degree of crystallinity. Ajji et Al. (32), who observed the same behaviour for roll-drawn and die-drawn PET, state that this behaviour is due to the transformation of some PET conformers from *gauche* to *trans*, which promotes crystal formation since only trans chains crystallise. The drawing also promotes crystallisation through alignment of the polymer chains. The crystallinity of their PET samples went from a crystallinity of 5% for undrawn samples to a crystallinity of 30% for samples drawn to a stretch ratio of 2.5 or higher.

Free-Blown Containers-Crystallinity and Stretch Ratio

Polypropylene

The experimental results indicated that the crystallinity of the membranes decreased as the blow time increased. Again, variations in the membrane's cooling rate are the main cause for this behaviour.

The variation in cooling rate originates from an increase in volume with increasing blow time, which decreased the wall thickness and increased the surface area exposed to the environment. Since all containers were formed from the same finite amount of material (i.e. a standard preform), the wall thickness decreased during inflation in order to compensate for the increase in length and width as illustrated in figure (2). For a unit volume V, a change in unit area L by L caused a change in the mean stretch ratio,

$$SR = \sqrt{\frac{1}{NORMALISED\ \ MEMBRANE\ \ THICKNESS}}$$

The crystallinity of the samples followed a linear change with thickness, also depicted on figure (2), agreeing with the theory that as the membrane became thinner, crystal growth was diminished due to an increase in cooling rate.

Polyethylene Terephthalate

The effect of varying the preform conditioning time prior to inflation and the blow time on the orientation and crystallinity of the resulting bubble was examined. The normalised membrane thickness was used instead of geometric mean of the hoop and axial stretch ratios as an indicator of orientation. The DSC results yielded similar crystallinities for the free blown samples as for the blow moulded samples, as indicated in figure 3. These results indicate that any effect that membrane thickness, conditioning time, blow mould temperature, and method of cooling within the range examined might have on crystallinity are all overshadowed by the effect of the stress imposed on the preform upon stretching, as described earlier for the blow moulded bottles.

Blow Moulded Containers-Permeability

Polypropylene

Results from the moulded bottles displayed a linear increase in permeability with increasing relative crystallinity at a constant stretch ratio. The variation in orientation caused by changes in shear rates due to a fluctuation in preform temperature during inflation was assumed to be negligible.

Polyethylene Terephthalate

The permeability coefficients for the blow moulded samples are represented in table 2. No major fluctuation in coefficient is noticeable within the range of conditions examined. There appears to be a slight increase in permeability with increasing blow mould temperature and increasing contact time but the minute change in values are inconclusive because of the lack of precision of the equipment used.

Table 2: Effect of blow mould temperature and mould contact time on bottle sidewall's relative crystallinity

		BLOW MOULD TEMPERATURE (Px10^{15}°C)			
		10	16	35	50
CONTACT TIME (s)	2	3.106	-----	-----	3.122
	4	-----	3.332	-----	3.180
	6	-----	-----	3.253	-----
	8	3.118	-----	-----	3.473

Assuming that this range of conditions bring forth no significant change in crystallinity or permeability, it can be concluded that extending blow mould contact time or increasing the mould temperature will not offer any advantageous properties that

cannot be found when operating at a more economical low mould temperature and exposure time.

Free-Blown Containers-Permeability

Polypropylene

The permeability analysis conducted on the free blown films provided a set of data that, unlike the blow moulded data, represented the permeability as a function of both crystallinity and stretch ratio. An increase in permeability with increasing crystallinity and decreasing stretch ratio was observed. Figure 4 separates the set of data between highly oriented and slightly oriented samples, and plots the resulting permeability coefficients as a function of crystallinity. For the highly oriented, (SR > 3.0), there appears to be a linear increase in permeability with increasing crystallinity, while the slightly oriented samples increase exponentially after reaching a minimum at approximately 85%. The formation of voids is suspected to be the cause of the upswing in permeability. This aspect will be discussed later in the report.

The permeability tests performed on the preforms produced higher readings than all membranes from free-blown and moulded bottle samples. This observation can be attributed to the fact that, unlike the bottles, the preforms are essentially cast polypropylene. In accordance with previous findings (33), the cast preforms were ~32% more permeable than the crystalline and oriented membranes taken from the bottles. The permeability coefficients of the preforms were therefore considered as being representative of an unstretched, 100% crystalline polypropylene sample.

Polyethylene Terephthalate

The permeability of the samples remained mostly constant for all free blown samples, but a slight decrease in permeability with increasing blow time. Both the preforms and blow moulded bottles offered a lower permeability to oxygen than the free blown bottles. The decrease in permeability cannot be attributed to crystallinity since both the free-blown bottles and the blow moulded bottles have approximately the same degree of crystallinity. It is important to note that all free blown bottles were tested with a 5 cm^2 mask while the blow moulded bottles were not. This may be the cause of the discrepancy between the values. Further testing should be performed to determine the cause of the variation in permeability between samples.

Table 3: Permeability of free blown samples compared with blow moulded bottle average and preform permeabilities

SAMPLE TYPE	FREE BLOW			BLOW MOULD (Avg.)	PREFORM
CONDITIONING TIME (s)	0	25	0	0	0
BLOW TIME (s)	0.15	0.3	0.5	2 to 8	0
PERM. COEFFICIENT	4.33 E-15	4.30 E-15	4.27E-15	3.23E-15	3.34E-15

Model Comparisons

2-Phase Model

All the data from the experiments was compiled and compared to the predictions obtained from the two phase model. This is illustrated on figure (5). It is clear to see that the experimental data and the prediction curve do not agree. A decrease in permeability with increasing relative crystallinity, as predicted by the 2 phase method, is not obeyed by the data.

An attempt was made to fit the 2-phase model to the experimental data. A linear fit of the experimental data was possible by taking the natural logarithm of equation (7), which yielded a linear equation,

$$LOG(P) = (b+1) \times LOG\left(\frac{(100 - Xc)}{100}\right) + LOG(P_{nc}) \qquad (16)$$

Where:

(b+1) = Slope of linear fit

LOG (P_{nc}) = Y intercept of linear fit

P_{nc} = 9.38e-13

The fit was attempted by fixing the value of P_{nc}, the permeability of the polymer at 100% amorphous content, as seen in figures (6) & (7) and then by letting P_{nc} be determined by the fitting process. These results are illustrated in figure (8) & (9). The method used to obtain the value of P_{nc} from data published by Weurth is explained later in the report.

Table 4: Comparison of Published values of Parameters & results from linear fit for 2-Phase model

	VALUE OF EXPONENT (b+1)	VALUE PERMEABILITY AT 100% AMORPHOUS CONTENT (P_{nc})
PUBLISHED VALUES	0.3 to 2.0	9.38E-13
RESULT OF FIT WITH FIXED P_{nc}	-1.3453	9.38E-13
RESULT OF FIT WITHOUT FIXED P_{nc}	-1.0163	1.1376E-13

The results from the linear fit of the 2 phase method to the experimental data proved to be poor. Although figure (9) offers a good representation of the data at high crystallinities, it loses accuracy as crystallinity decreases. For this, the 2 phase model would probably produce erroneous results if attempts were made to predict the shelf life of an ISBM container.

Permacor Model

The permacor method as presented by Salame (17) can be used for permeability predictions of unstretched materials as well as films stretched to a draw ratio of ~2.5. The absence of stretch ratio in the equation of permeability which limited the use of the model. Equation (9) was modified to take the stretch ratio into account with the use of the data points provided by Salame to fit the form,

$$P = \left(\frac{A}{(\alpha_1 \phi + \alpha_2) \times \left(\frac{(100 - Xc)}{100} \right)^{(\gamma_1 \phi + \gamma_2)}} \right) e^{-s\pi} \qquad (17)$$

Where,

ϕ = Stretch ratio of the sample

$\gamma_{1,2}$ = Coefficients determined through linearisation

$\alpha_{1,2}$ = Coefficients determined through linearisation

The data provided by Salame was value of τ_o at stretch ratios of 1 and ~2.5.

Table 5: Data provided by Salame

STRETCH RATIO (ϕ)	γ	α
1.0	0	1
2.5	1.13	-0.5

These were enough to solve for the parameters α_1, α_2, γ_1 and γ_2 ,

Table 6: Coefficients for adjusted Permacor model

PARAMETER	γ_1	γ_2	α_1	α_2
VALUE	-0.333	0.333	0.0867	0.9133

The prediction of permeability from this modified Permacor equation is compared to experimental data on figure (10). Once again, the model fails to follow the increasing trend in permeability at high crystallinity.

Best-Fit Model

Since no existing models adequately represented the experimental data, attempts were made to fit linear, exponential and polynomial equations to represent the permeability coefficient of a membrane as a function of relative crystallinity and stretch ratio of the ISBM part.

The range of experimental data was from 78 % to 100 % crystalline and the stretch ratio tested was from 1 to 6.5. Literature was searched for data to help in fitting and extrapolating of equation. Such a value was reported by Salame, who had a permeability of ~1.35e-13 for polypropylene at 60% relative crystallinity.

Another important point sought was the permeability of amorphous polypropylene. Weurth (9) reported values for diffusivity and solubility of Helium in atactic polypropylene, taken as the analogue of amorphous polypropylene. Using the relative permeability parameters conversion table for different gases from Van Krevelen (34) and equation (3), a data point was obtained. Since this number was not the direct result of a test of the permeability of oxygen through polypropylene, this point was not used in the fitting process.

A polynomial model proved to be the best-fit equation to the experimental data. The following polynomial was fitted,

$$P = d + e \times (\phi - 1) + f \times (\phi - 1)^2 + g \times \left(\frac{(100 - Xc)}{100}\right) + h \times \left(\frac{(100 - Xc)}{100}\right)^2 \quad (18)$$

Where,
P = Permeability Coefficient
ϕ = Mean Stretch Ratio
Xc = Relative Crystallinity (%)
d, e, f, g ,h = Equation Parameters

The equation parameters resulting from the fitting process are:

Table 7: Equation parameters for Polynomial Equation

PARAMETER	*BEST-FIT VALUES FOR POLYNOMIAL EQUATION*	*STANDARD ERROR*
d	1.510E-13	30.05E-15
e	-1.8336E-15	1.953E-15
f	1.0967E-16	3.598E-16
g	-5.383E-13	2.55E-14
h	1.3804E-12	6.166E-14

A planar view of the fit, relating relative crystallinity and stretch ratio to the permeability coefficient is plotted on figure (11), while figure (12) displays the fitted results in two dimensions. It is important to keep in mind that very large extrapolations with a limited amount of data points are questionable and therefore may lose some validity over the entire curve. To test the exactness of the extrapolation, the data point for 100% amorphous polypropylene calculated from Weurth's findings was compared to the polynomial's prediction.

Table 8: Comparison of exper imental permeability of polypropylene to prediction from extrapolated polynomial

	EXPERIMENTAL DATA FROM WEURTH (8)	*THEORETICAL PREDICTION FROM POLYNOMIAL EXTRAPOLATION*
PERMEABILITY OF 100% AMORPHOUS POLYPROPYLENE	9.38E-13	9.93E-13
	Percent Error = 5.7 %	

The fit appears to be acceptable, but should be subjected to a validation process to evaluate its worth. This includes testing at different thickness, crystallinity and stretch ratio combinations.

It is important to note that all models displayed a decrease in permeability with increasing stretch ratio. The polynomial model appeared to be the model least affected by changes in stretch ratio. The accuracy of the stretch ratio could not be evaluated due to a lack of data.

The results from the previously published models and the polynomial fit are evidently conflicting in the upper range of crystallinities. The increasing trend in the experimental data at high levels of crystallinity tends to indicate that as the crystalline concentration increases, the passage of oxygen through the membrane is facilitated. Wuerth (9) observed that the diffusion of different gases (Helium, Argon and CF_4) in highly crystalline (60%-100%) polypropylene followed the same trend as the experimental data. To determine if the observation from this study was in accordance with Wuerth's findings, the solubility equation derived by Salame (17),

$$S = \varphi e^{-\beta\pi - 0.013(\varepsilon/k)} \qquad (19)$$

Where:S = Solubility coefficient

$\varphi = 6.8 * 10^{-3}$ and $\beta = 0.030$

(ε/k)=Lennard-Jones Potential of penetrant

was divided from permeability coefficients corresponding to relative crystallinities ranging from 0% to 100% as calculated with the polynomial fit. The resulting set of diffusion coefficients at a stretch ratio of 1 is depicted in figure (13). Weurth's diffusion plots are found on figures (14), (15), & (16). Although the diffusion plot

originating from the polynomial fit has different units that the other figures, it appears that the diffusion pattern followed by the ISBM samples is the same as for Weurth.

Vieth (10) theorizes that the increase in diffusion as crystalline content increases can be caused by non-interconnected defects passing through individual lamellae , rendering some crystallites semi-permeable. This in turn results in a decrease in the final tortuose path length. This formation of defects is caused by the thickening of the lamellae upon slow cooling. During thickening, it occasionally happens that a lamella pulls a chain into its structure, creating a vacant row. This phenomenon must only occur in a small fraction of the polymer to account for the increase in diffusivity.

The major difference between the Weurth's findings and those presented here are that the former subjected his samples to controlled annealing conditions while the samples used in the present experiments resulted from standard stretch blow moulding processing conditions. The high levels of crystallinity of the samples seemed to indicate that the cooling pattern of the bottles is a slow process, permitting the lamellae to thicken, producing defects within the film to facilitate gas diffusion. Microscopic and column density analyses should be conducted to evaluate the validity of this hypothesis.

Conclusion and Recommendations

The characterization of stretch-blow moulded polypropylene displayed an increase in permeability with increasing crystallinity and decreasing stretch ratio over the range of crystallinity and stretch ratio studied. Existing models to predict permeability such as the 2 phase model and the Permacor method were compared to the experimental data. The models failed to follow the same trend as the data in the upper range of crystallinity, rendering them inadequate for eventual shelf life predictions. A polynomial equation proved to fit the data the best, despite the mediocre representation of the effect of orientation on final permeability. The extrapolation of the equation seemed to offer a fair representation of published data.

Potential future work includes:

- Microscopy testing on polypropylene samples to verify the hypothesis of void formation within the polymer's crystalline structure which causes permeability to increase with crystallinity.
- Widen test range for PET and PP to obtain more data.
- Validation through integration of barrier models into a simulation program to predict a container's performance after processing.
- Similar study with other polymers, such as PC and PET/PEN blends.

References

1. Fick, A., Ann. Physik, **94**, 59 (1955)

2. Wang, L.H., Porter, R.S., On the CO_2 Permeation of Uniaxially Drawn Polymers, J. Polym. Sci., **22**, 1645-1653, (1984)

3. Webb, J.A., Bower, D.I., Ward, I.M., Cardew, P.T., The Effect of Drawing on the Transport of Gases through Polyethylene, J. Polym. Sci., **31**,743-757 (1993)

4. Ciora Jr., R.J., Magill, J.H., Novel Rolltruded Films. II. Effect of Draw Ratio on the Transport Properties of Rolltruded Isotactic Poly(propylene), J. Polym. Sci., **32**, 305-312 (1994)

5. Swaroop, N., Gordon, G.A., Transport in Oriented Bottles Made from Polyester Resins, Polym. Eng. Sci., **20**, 1, 78-81, (1980).

6. Magill, J.H., Rate of Crystallization of Polymers, Polymer Handbook, 3rd Edn., Eds. J. Brandrup and E.H. Immergut , Wiley-Interscience, New York, **VI**, 279, 1989.

7. Patell, R.M., Spruiell, J.E., Crystallization Kinetics During Polymer Processing-Analysis of Available Approaches for Process Modelling, Polym. Eng. Sci., **31**, 10, 730-738 (1991)

8. Aubert, R., DiRaddo, R. , Laroche, I., Modelling, Experimental Validation and Material Characterization of Solidification Dynamics in Blow Moulding, NRC, April, 1996.

9. Weurth, W.F., A Study of Poly(Propylene) by Gas Permeation, Sc. D. Thesis in Chemical Engineering, Mass., Institute of Technology, 1968

10. Vieth, W.R., Diffusion In and Through Polymers: Principles and Applications, Hanser Publishers, New York, 1991, chap. 4

11. Perkins, W., Effect of Molecular Weight and Annealing Temperature on the Oxygen Barrier Properties of Oriented PET film, Polym. Bull., **19**, 397-401, (1988)

12. Kim, S.L., Effect of Preheat Time on the Morphological and Oxygen Barrier Properties of Reheat Blown PET Containers, Polym. Eng. Rev. **4**, 4, 239-254, (1984)

13 Leigner, F.P., Freeblowing PET Preforms, ANTEC '85, 907-911, (1985)

14. Venkateswaran, G., Jabarin, S.A., Effects of Moisture and Physical Aging on the Free Blow Characteristics of PET, ANTEC '96, 943-952, (1996)

15 . Comyn, J., Polymer Permeability, Elsevier Applied Science Publishers, London, 1985, p.65.

16. Gohil, R.M. , Morphology - Permeability Relationships in Biaxially Oriented Pet Films: A Relationship Between Oxygen Permeability and PROF, J. App. Polym. Sci., **48**, 1649-1664, (1993).

17. Salame, M., Prediction of Gas Barrier Properties of High Polymers, Polym. Eng. Sci., **26**, 22, 1543-1546, (1986)

18. Bicerano, J., Prediction of Polymer Properties., Marcel Dekker Inc., New York, 1993, Chapt. 15.

19. Jia, L., Xu, J., A Simple Method for Prediction of Gas Permeability of Polymers from Their Molecular Structure, Polym. J., **23**, 5, 417-427, (1991).

20. Kit, K.M., Schultz, J.M., Gohil, R.M., Morphology and Barrier Properties of Oriented Blends of Poly (Ethylene Terephthalate) and Poly(Ethylene 2,6-Naphthalate) with Poly(Ethylene-co-Vinyl Alcohol), Polym. Eng. Sci., **35**, 8, 680-692, (1995).

21. Robertson, G.L., Food Packaging: Principles and Practice, Marcel Dekker Inc., New York, 1993, p.92

22. Shires, D., Developments in Barrier Technology, Pira reviews of Packaging, Pira International, 1993, p.27.

23. Pauly, S. Permeability and Diffusion Data. In Polymer Handbook, 3rd Edn., J. Brandrup and E.H. Immergut (Eds.), Wiley-Interscience, New York, 1989, Section VI.

24. D.C.S.T., Utilisation des plastiques en emballage alimentaire, National Library, 1st trimester, 1994, p.64.

25. Rogers, C.E., In: Physics and Chemistry of the Organic Solid State, Vol.2, eds. Fox, D., Labes, M.M., Weissberger, A., Interscience Publ., New York, 1965, chap. 6.

26. Crank, J., Park, G.S., Diffusion in Polymers, Academic Press, New York, 1968.

27. Sobolev, J.A., Stannett, V., Szwarc, M., Ind. Engr. Chem., 49, 441 (1957).

28. Michaels, A.S., Parker, R.B., J. Polym. Sci., 41, 53 (1959)

29. Jasse, B., Seuvre, A.M., Mathlouthi, M., In: Food Packaging and Preservation, Ed. Mathlouthi, M., Blackie Academic and Professional, New York, Chap. 1, (1994)

30. Rosato, D.V., Rosato, D.V., Blow Molding Handbook, Hanser Publishers, New York, 1989, p. 552.

31. Mehta, A., Gaur, U., Wunderlich, B., Equilibrium Melting Parameters of Poly(ethylene Terephthalate)., Journal of Polymer Science: Polymer Physics Edition, 16, 289-296, (1978).

32. Ajji, A., Cole, K.C., Dumoulin, M.M., Orientation of Amorphous Polyethylene Terephthalate by Tensile Drawing, Roll-Drawing and Die-Drawing., Antec '97

33. Benning, C.J., Plastic Films For Packaging: Technology, Applications and Process Economics, Technomic Publishing Co. Inc., Pennsylvania, 1983, p.43.

34. Van Krevelen, , Properties of Polymers: Their Correlation with Chemical Structure: Their Numerical Estimation and Prediction from Additive Group Contributions, Elsevier Science Publishers, 3rd Ed., 1990, p.555.

Nomenclature

A	Gas constant for Permacor method
b	Equation parameter dependent on polymer
c	Penetrant concentration
d	Equation parameter
D	Diffusivity coefficient
D_{nc}	Diffusivity coefficient of 100% amorphous polymer
e	Equation parameter
f	Equation parameter
g	Equation parameter
h	Equation parameter
J	Diffusive flux of Penetrant
l	Thickness of membrane
p	Partial pressure of diffusing gas
P	Permeability coefficient
P_{nc}	Permeability coefficient of 100% amorphous polymer
s	Gas constant for Permacor method
S	Solubility coefficient
S_{nc}	Solubility coefficient of 100% amorphous polymer
x	Membrane thickness
Xc	Relative crystallinity
$\alpha_{1,2}$	Equation parameter
$\gamma_{1,2}$	Equation parameter
π	Permacor adjusted for crystalline content
π_a	Permacor value
τ_o	Tortuosity caused by orientation of crystallites
ΔH_f	Enthalpy of sample
$\Delta^* H_f$	Enthalpy of 100% crystalline polymer
ϕ	Stretch ratio of sample
φ	Equation parameter determined by Salame
β	Equation parameter determined by Salame
(ε/k)	Lennard-Jones Potential of penetrant

List of Captions

RELATIVE CRYSTALLINITY vs. BLOW TIME FOR BLOW MOULDED BOTTLES AT DIFFERENT COOLING CHANNEL TEMPERATURES

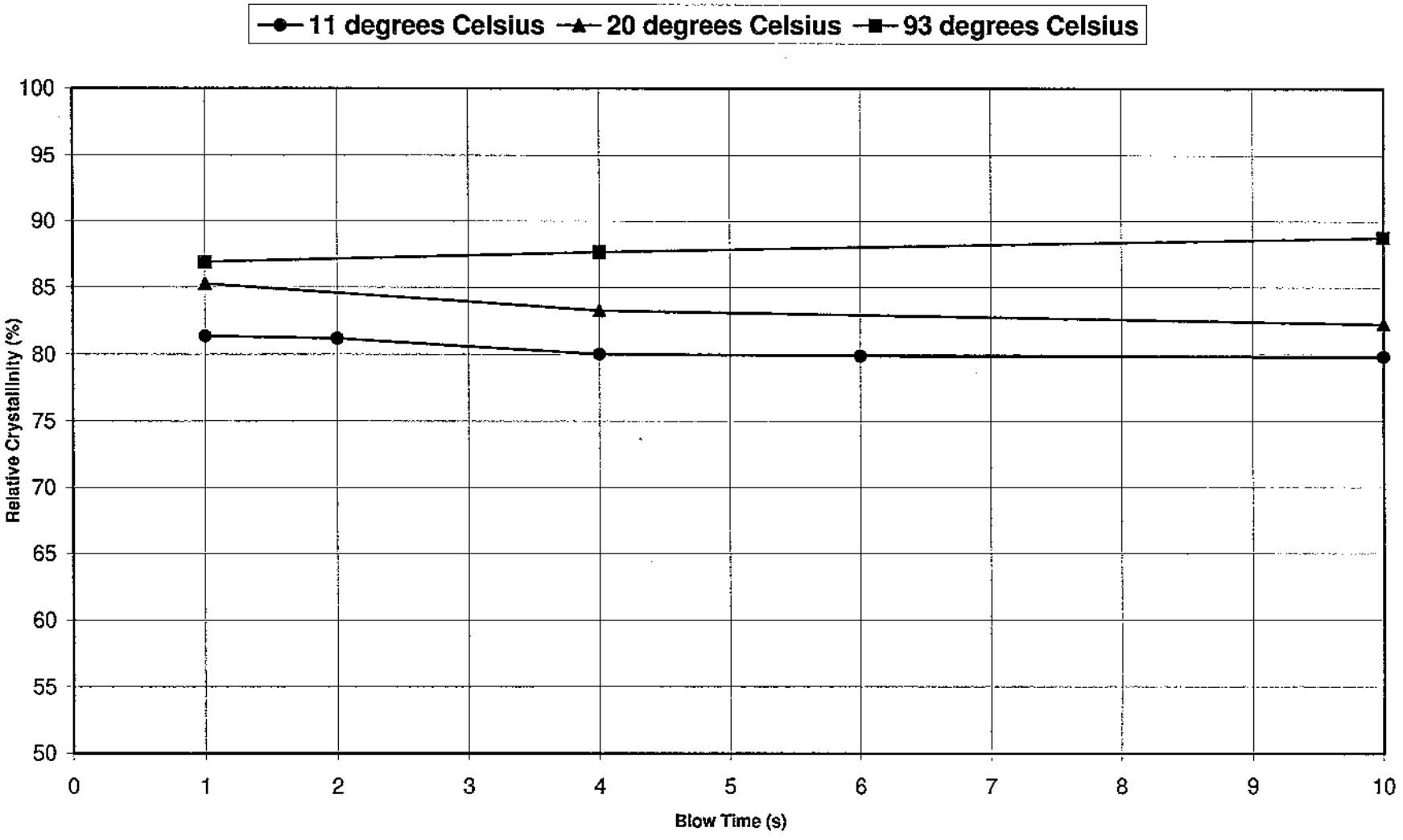

FIGURE 1: Relative Crystallinity as a function of blow time for blow moulded bottles at different mold cooling channel temperatures

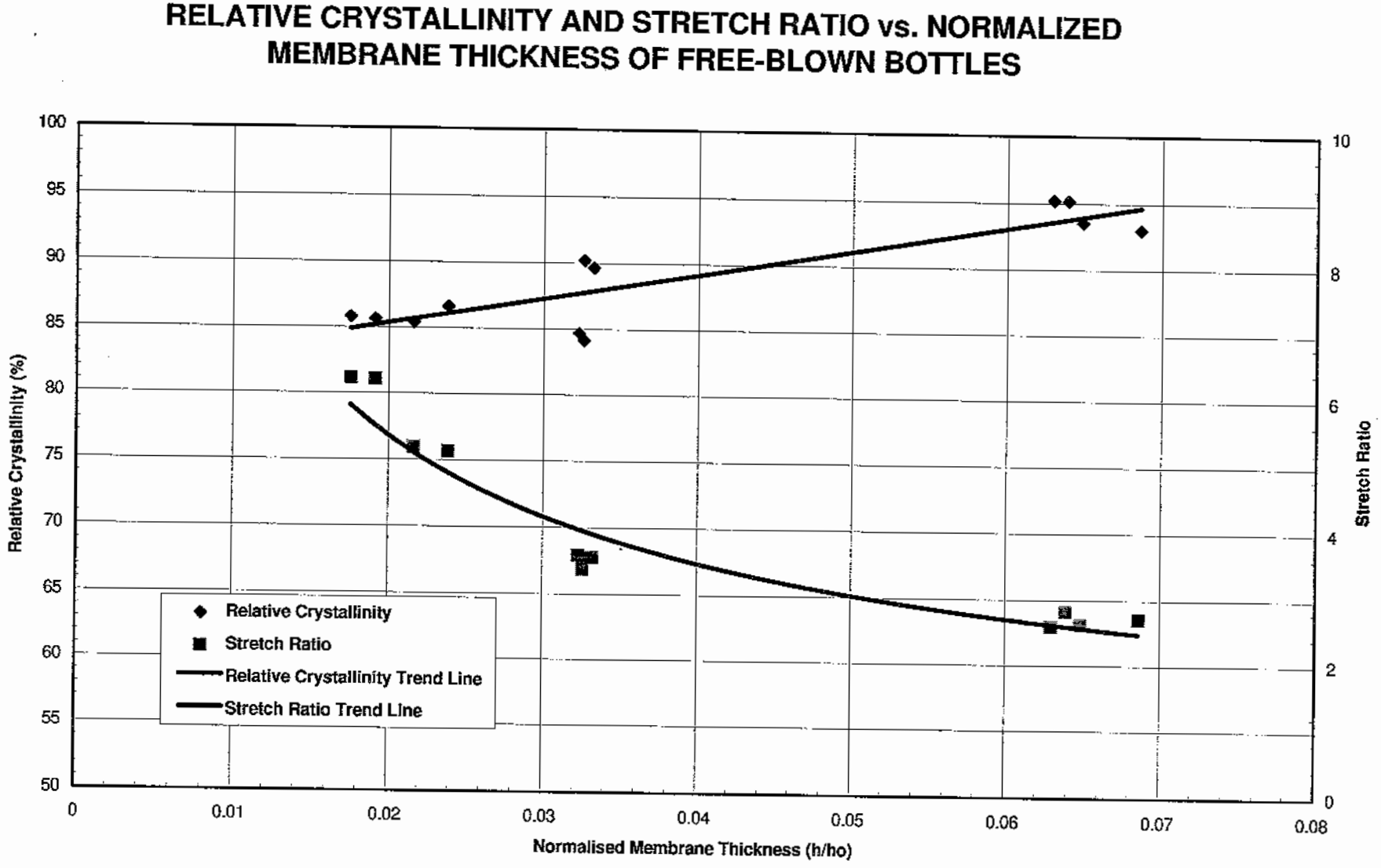

FIGURE 2: Relative Crystallinity and Stretch Ratio vs. normalised membrane thickness of free-blown bottles

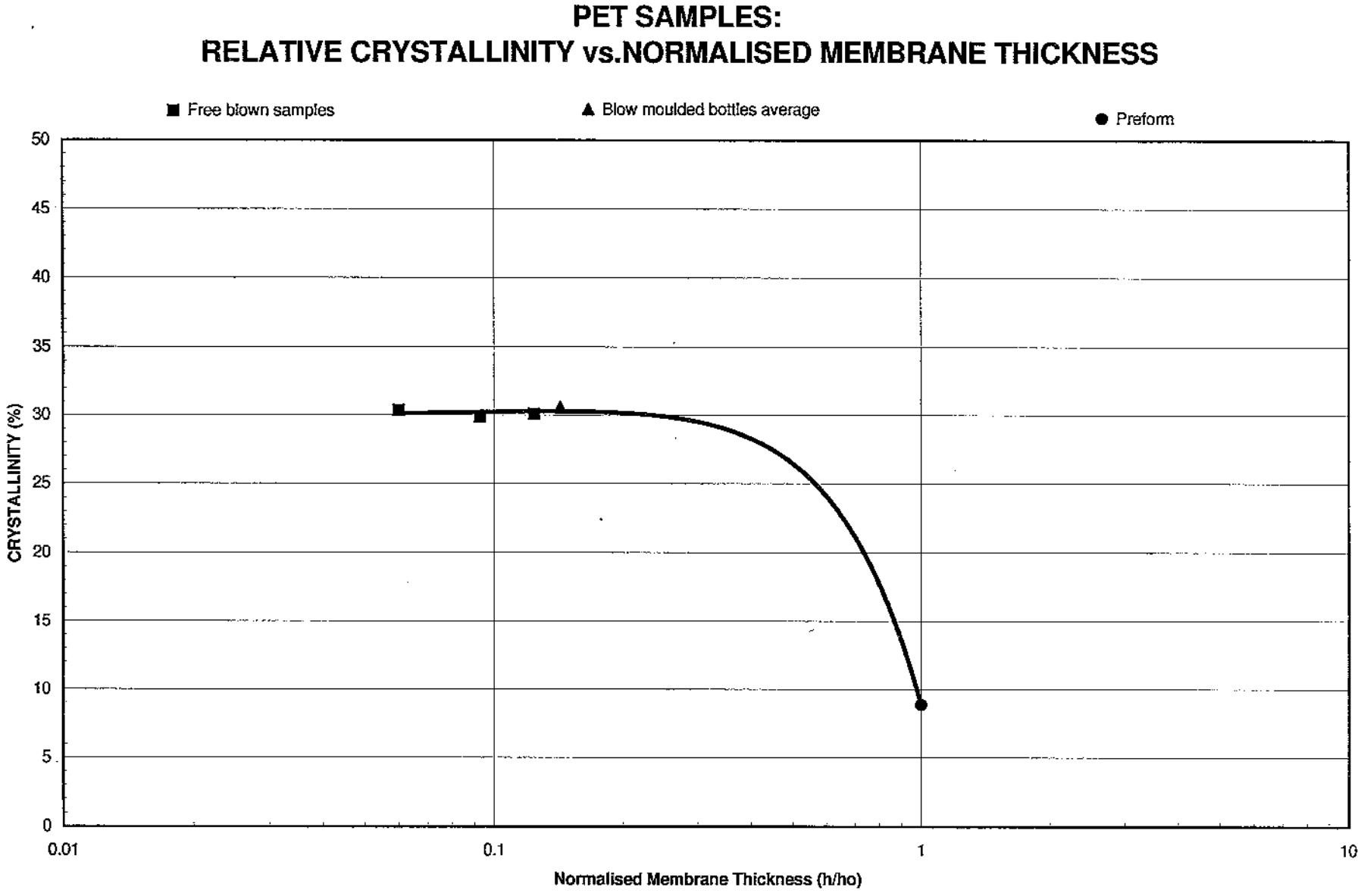

FIGURE 3: Relative crystallinity of PET samples as a function of the normalised wall thickness

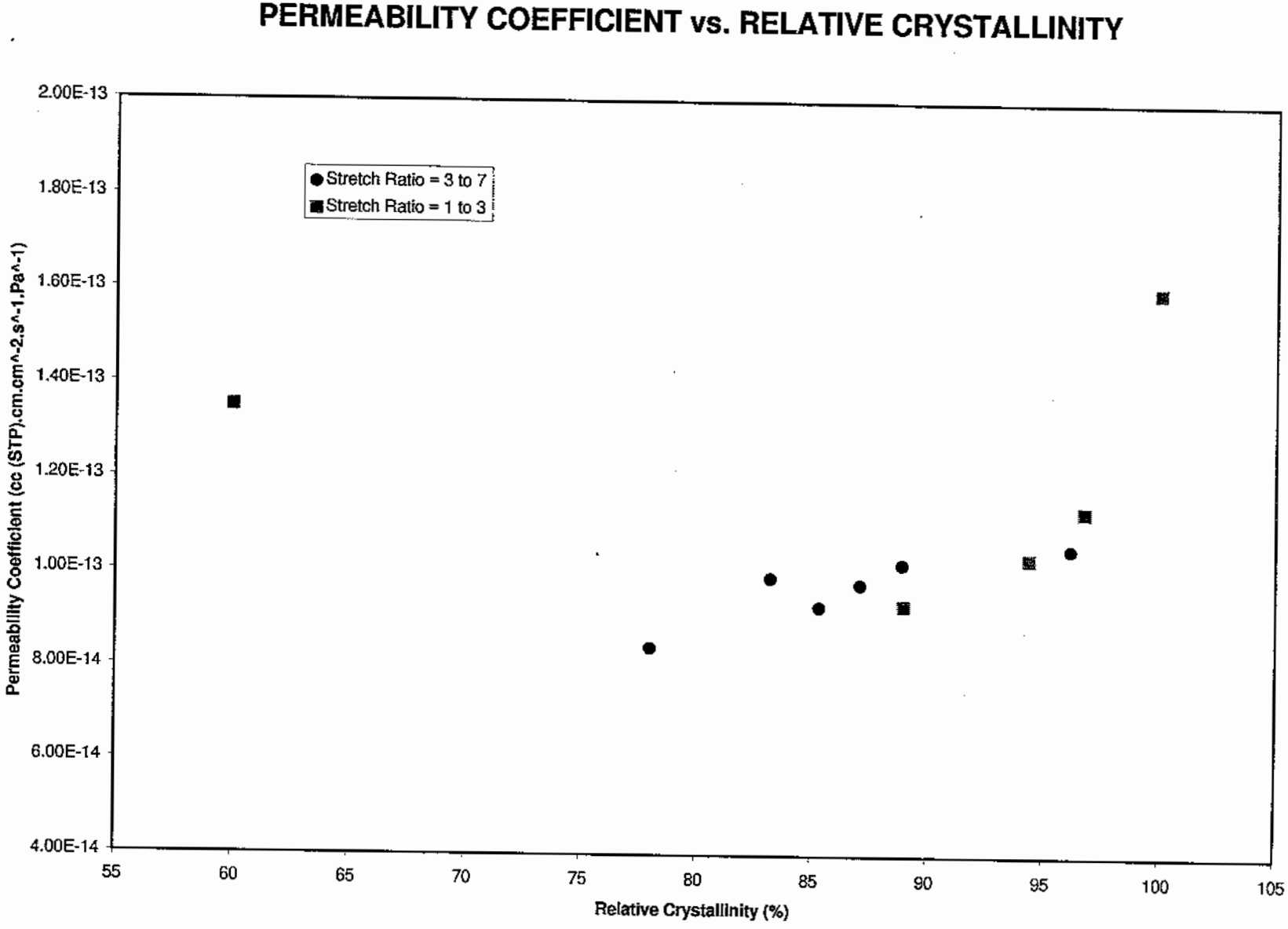

FIGURE 4: Permeability coefficient of PP with respect to relative crystallinity at highly (SR > 3) and slightly (SR < 3) oriented levels.

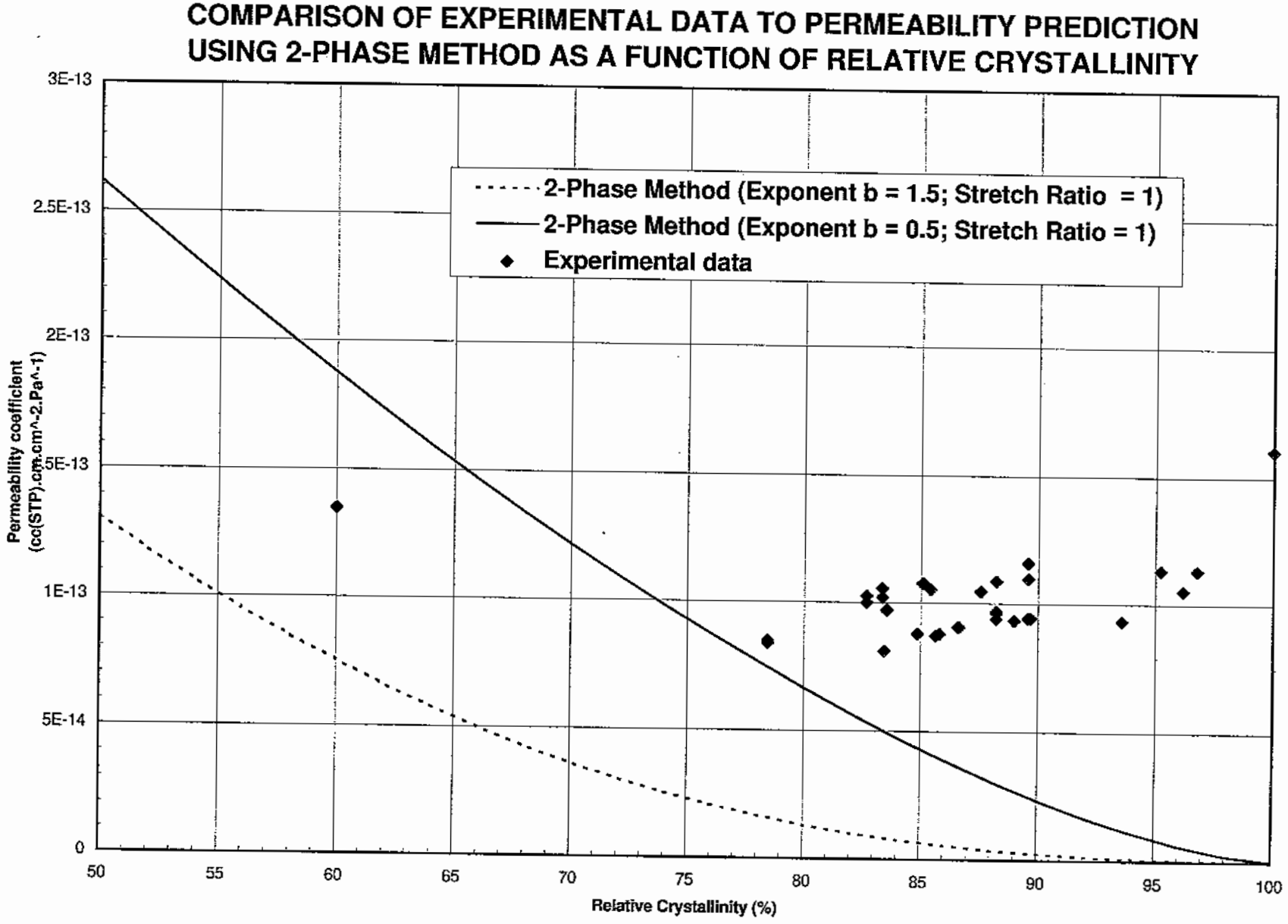

FIGURE 5: Comparison of Experimental Data to Permeability Prediction Using 2-Phase method as a function of Relative Crystallinity

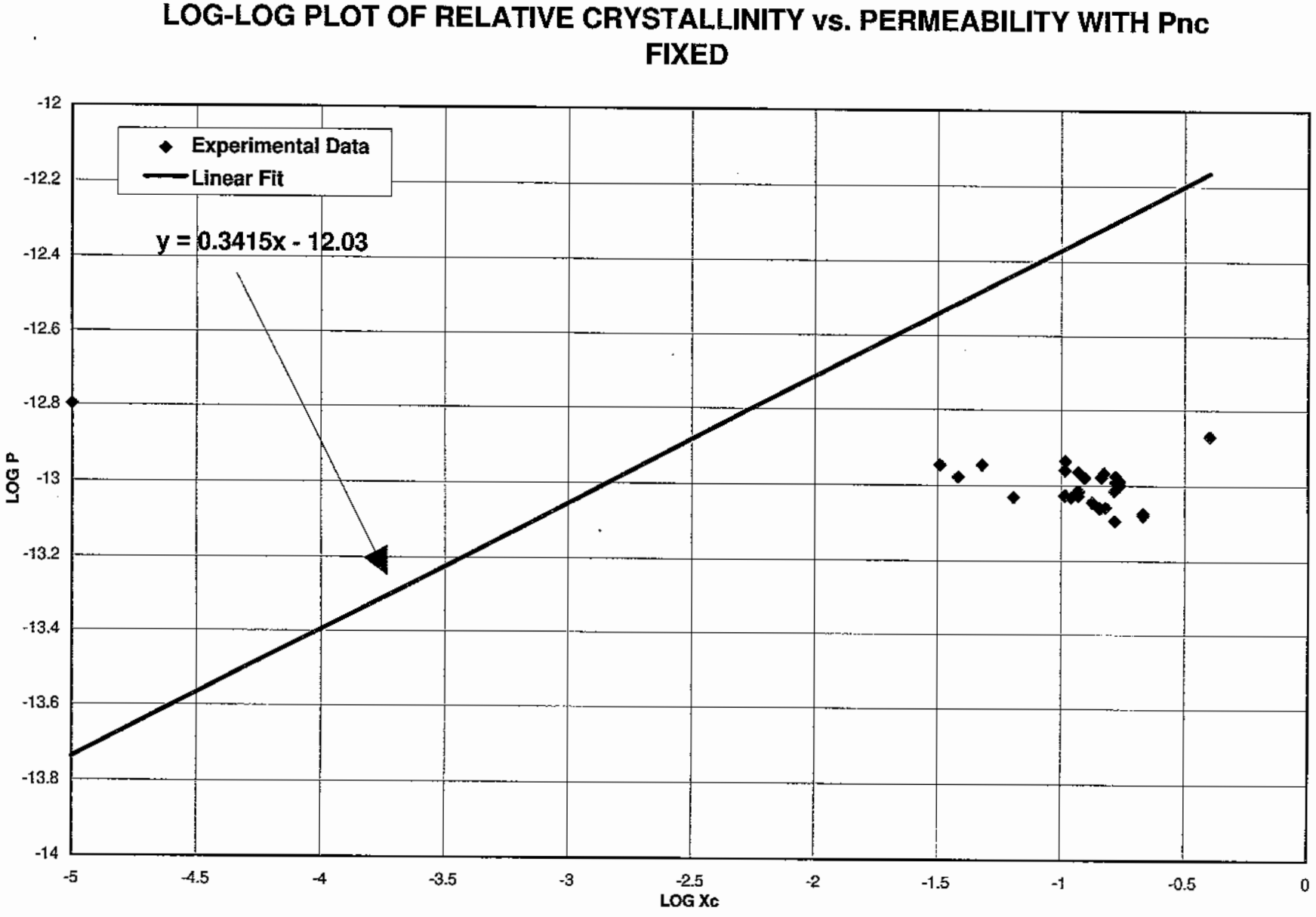

FIGURE 6: Logarithm of permeability vs. the logarithm of Relative Crystallinity with 100% amorphous permeability fixed at 9.38E-13

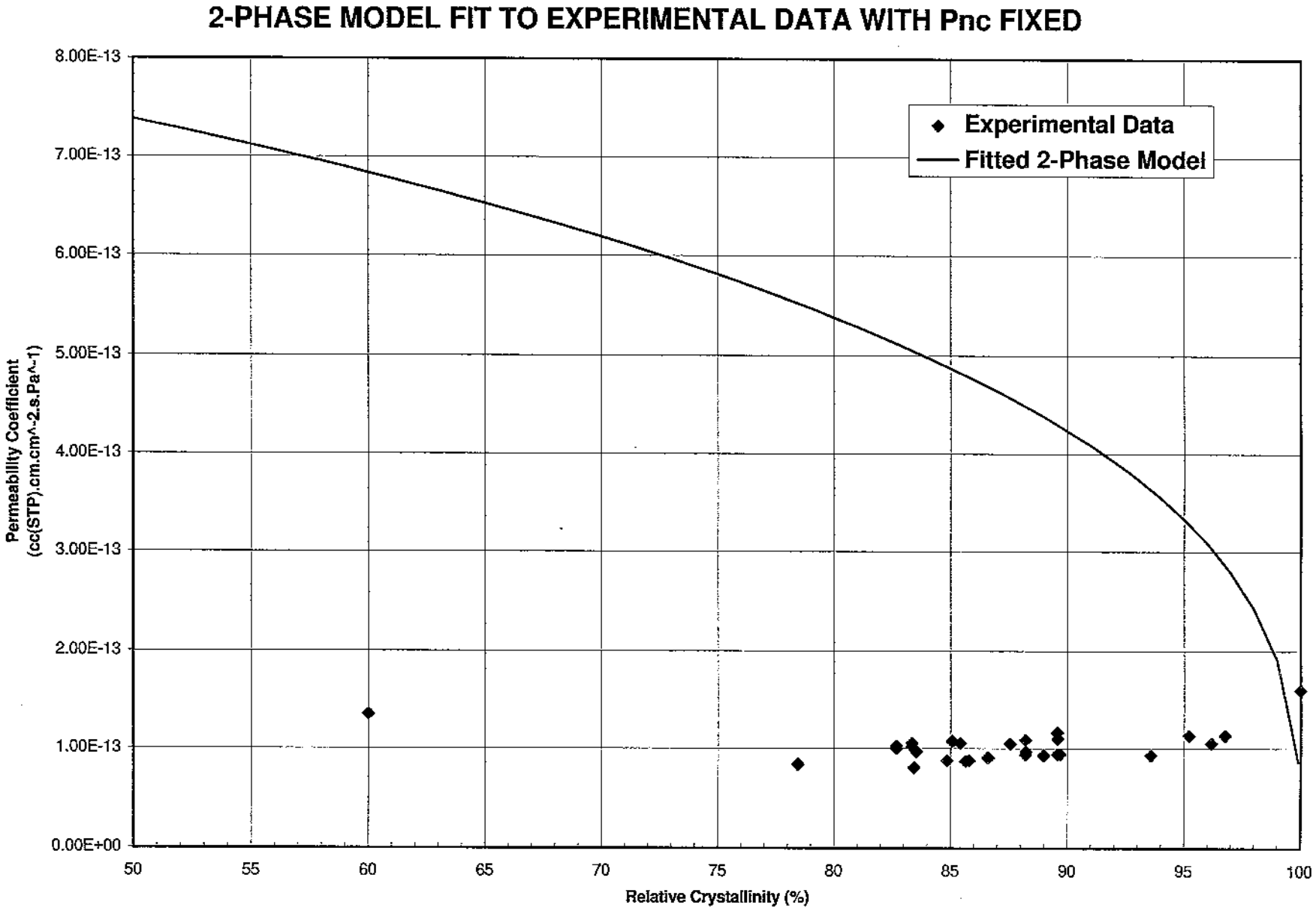

FIGURE 7: 2-phase model fit to experimental data with Pnc Fixed

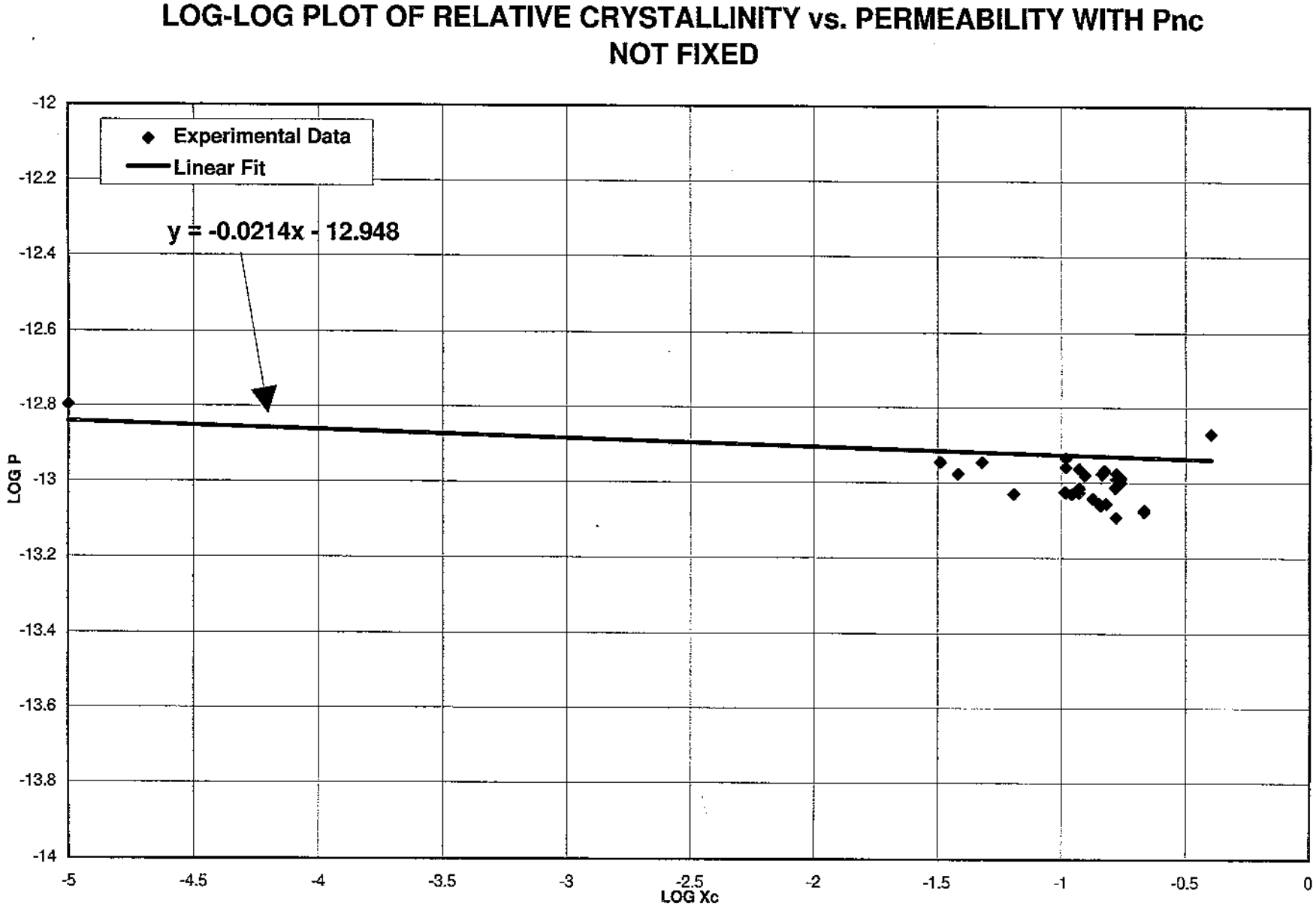

FIGURE 8: Logarithm of permeability vs. the logarithm of Relative Crystallinity with 100% amorphous permeability not fixed

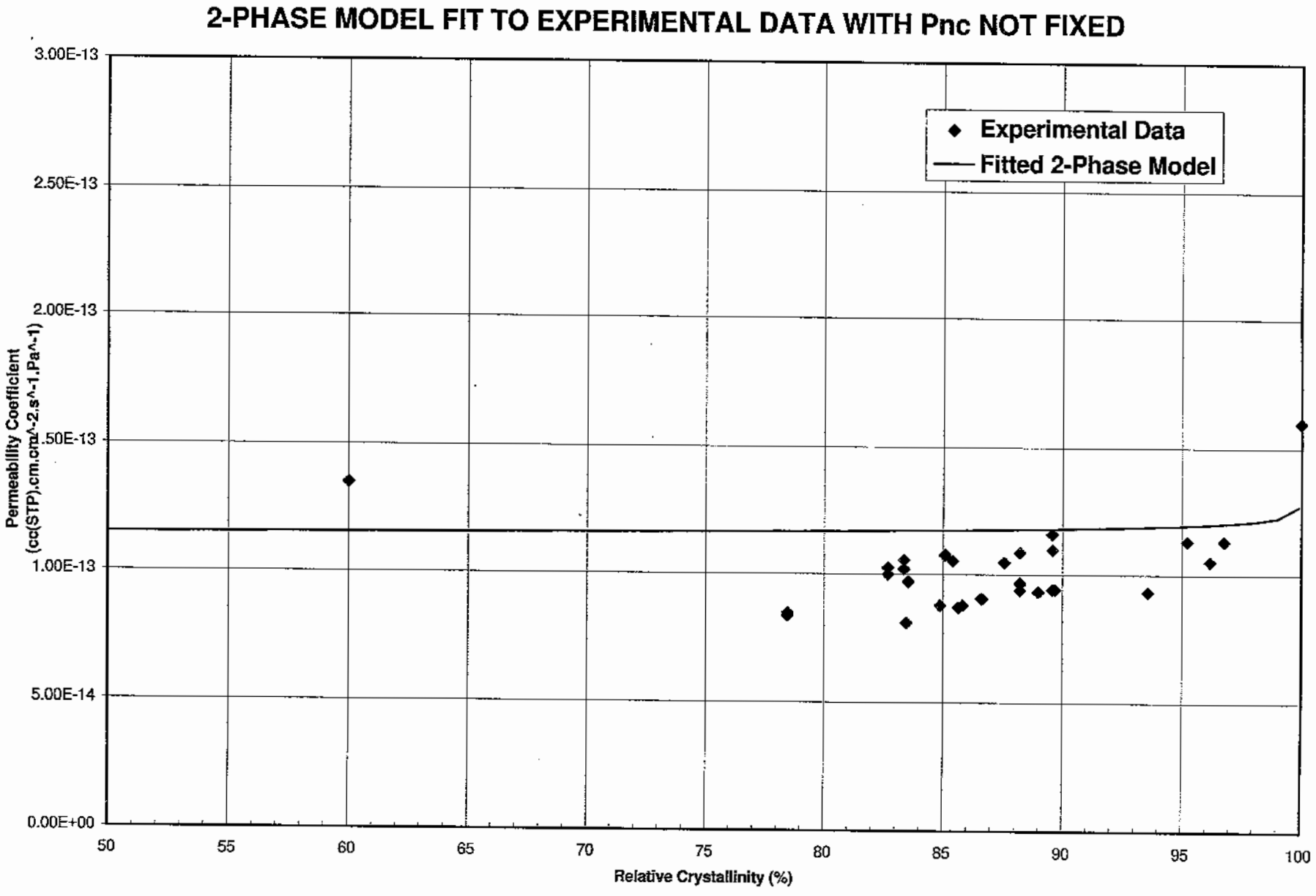

FIGURE 9: 2-Phase model fit to experimental data with Pnc not fixed

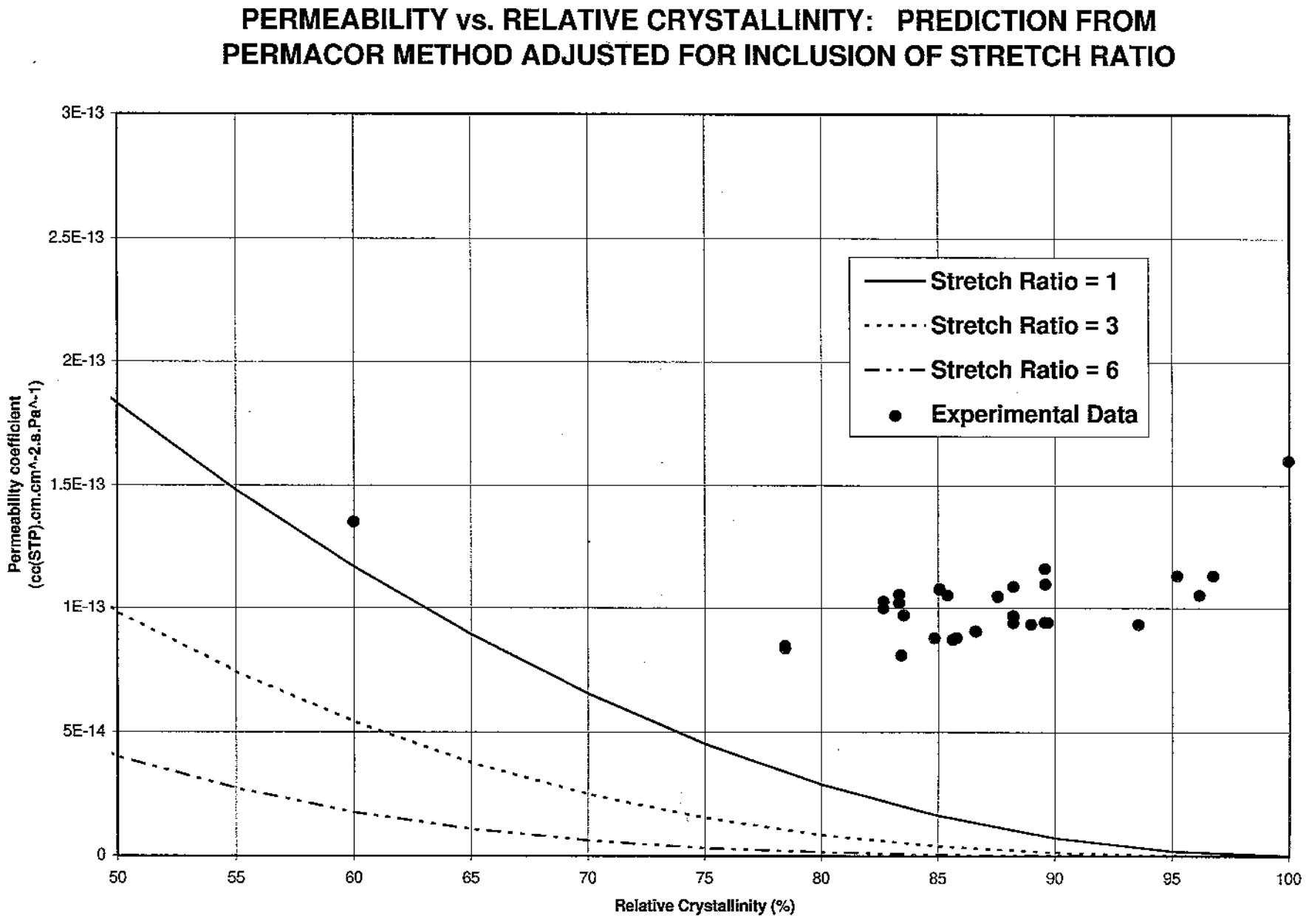

FIGURE 10: Comparison of Experimental Data to Permeability Prediction using the Permacor method modified to include stretch ratio

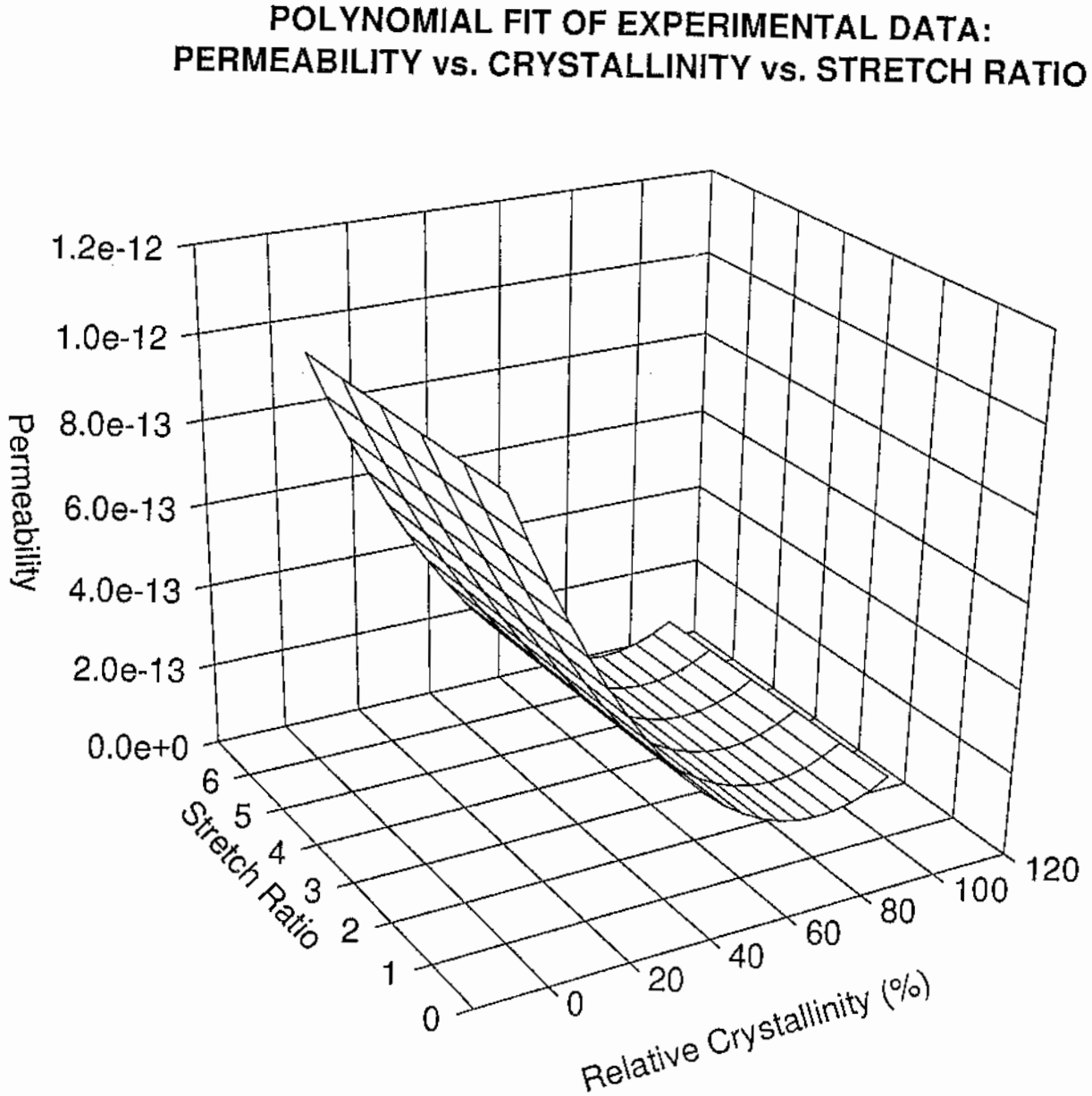

FIGURE 11: Polynomial Fit of experimental data in 3D space: Permeability as a function of relative crystallinity and stretch ratio.

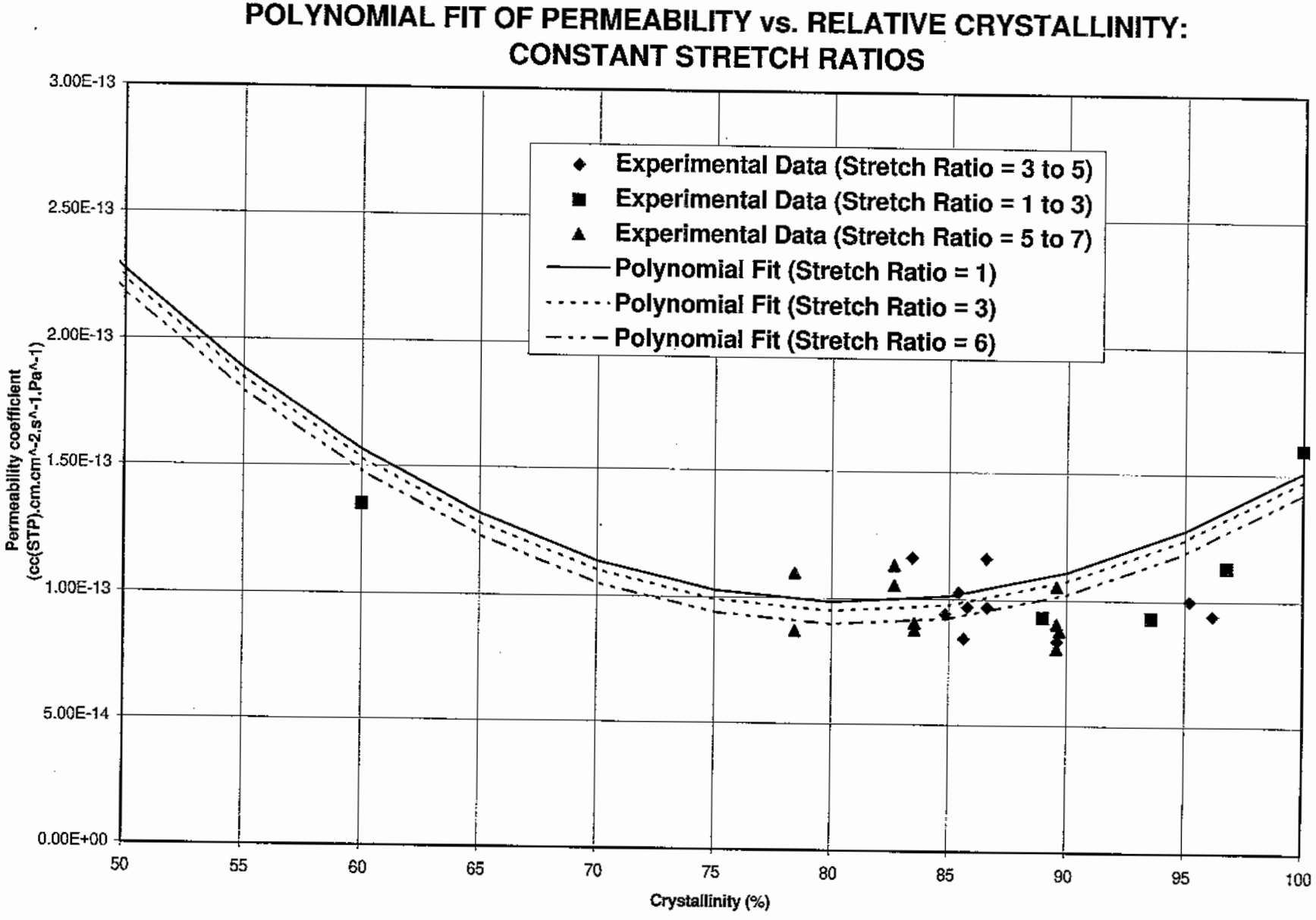

FIGURE 12: Polynomial fit of experimental data: Permeability vs. Relative Crystallinity at different Stretch Ratios

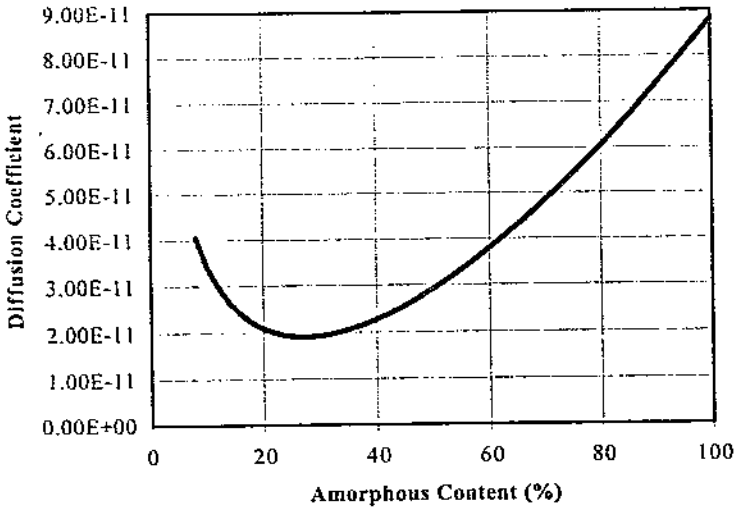

FIGURE 13: Diffusivity coefficient of O_2 from polynomial model vs. amorphous content (Note: Although units are different, the same trend is evident)

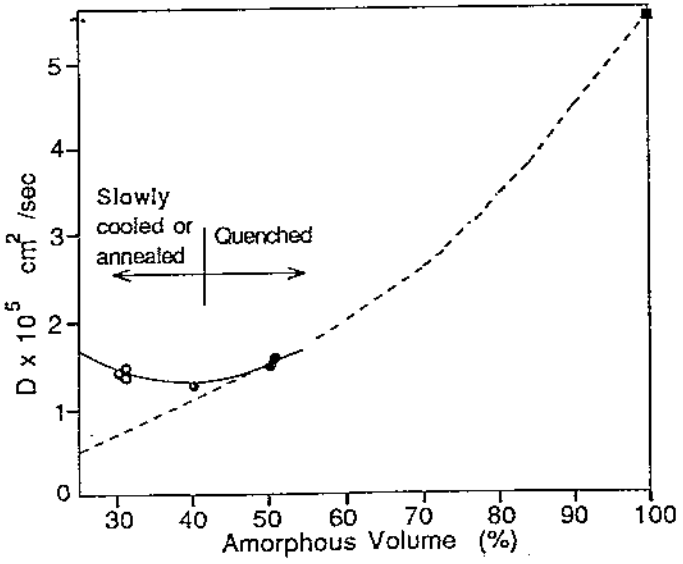

FIGURE 14: Diffusivity coefficient of Helium from Weurth (8) vs. amorphous content

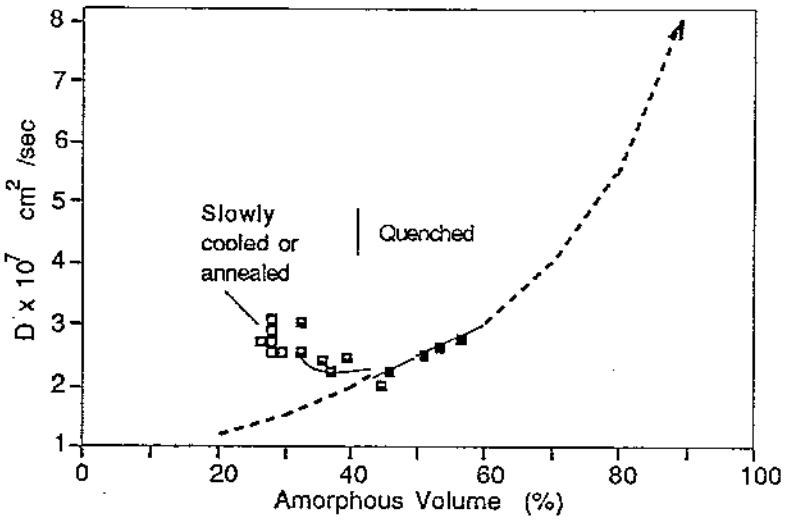

FIGURE 15: Diffusivity coefficient of Argon from Weurth (8) vs. amorphous content

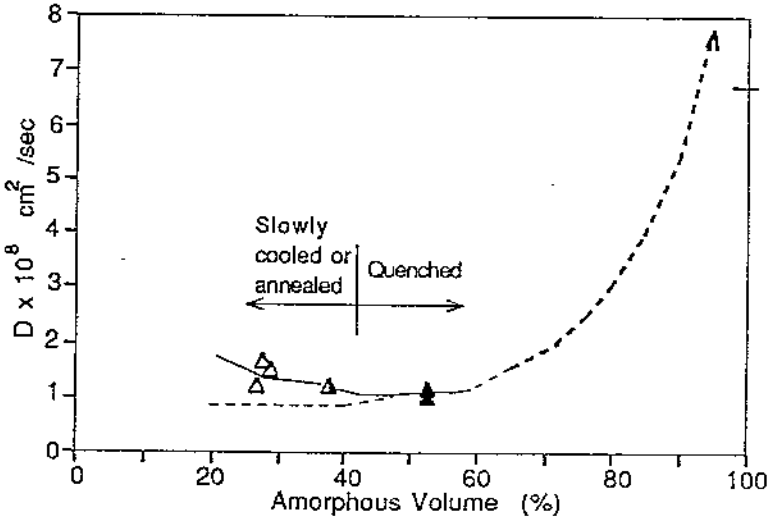

FIGURE 16: Diffusivity coefficient of CF_4 from Weurth (8) vs. amorphous content

EXPERIMENTAL DATA:

	SR	Xc	P	Weight
	2.598	95.21	1.13265E-13	1
	2.627	93.57	9.32241E-14	1
Data	5.191	85.41	1.05297E-13	1
	5.128	86.63	9.04974E-14	1
	6.237	85.80	8.7768E-14	1
	6.214	85.64	8.07735E-14	1
from	3.5621	89.47	9.41166E-14	1
	3.56	89.69	1.16087E-13	1
	2.598	96.76	1.13265E-13	1
	2.627	88.98	9.32241E-14	1
Freeblown	5.191	96.17	1.05297E-13	1
	5.128	88.60	9.04974E-14	1
	6.237	84.86	8.7768E-14	1
	6.214	83.44	8.07735E-14	1
Bottles	3.5621	89.57	9.41166E-14	1
	3.56	89.73	1.16087E-13	1
	5.067	89.59	1.09816E-13	1
	3.73	82.68	9.86784E-14	1
Data	3.73	82.68	1.02572E-13	1
	3.73	83.54	9.69069E-14	1
	3.73	83.54	9.71039E-14	1
	3.73	78.45	8.44809E-14	1
from	3.73	78.45	8.34939E-14	1
	3.73	89.22	9.3865E-14	1
	3.73	88.22	1.08808E-13	1
	3.73	85.08	1.07568E-13	1
Moulded	3.73	85.08	1.0783E-13	1
	3.73	83.35	1.02076E-13	1
	3.73	83.35	1.05626E-13	1
	3.73	88.22	9.62844E-14	1
Bottles	3.73	88.22	9.67897E-14	1
	3.73	87.56	1.04656E-13	1
	3.73	87.56	1.04847E-13	1
	1	100.00	1.21127E-13	1
Data	1	100.00	2.72535E-13	1
	1	100.00	1.1608E-13	1
from	1	100.00	1.35258E-13	1
	1	100.00	2.01878E-13	1
Preforms	1	100.00	4.31009E-13	1
	1	100.00	3.18967E-13	1
from Salame	1	60.00	1.35E-13	39

EQUATION PARAMETERS:

d	1.5100E-13
e	-1.8336E-15
f	1.0967E-16
g	-5.3630E-13
h	1.3604E-12

EQUATION (Polynomial):

Z=d+e*(SR-1)+f*(SR-1)^2+g*((100-Xc)/100)+h*((100-Xc)/100)^2

RESULTS FROM EXTRAPOLATED DATA WITH EQUATION

STRETCH RATIO

Xc (%)	1	5	10	15	20
0	9.931E-13	9.8752E-13	9.8548E-13	9.89E-13	9.97852E-13
5	8.85426E-13	8.79848E-13	8.7781E-13	8.81E-13	8.90178E-13
10	7.84654E-13	7.79074E-13	7.7703E-13	7.8E-13	7.89406E-13
15	6.90784E-13	6.85204E-13	6.8316E-13	6.87E-13	6.95536E-13
20	6.03816E-13	5.98236E-13	5.962E-13	6E-13	6.08568E-13
25	5.2375E-13	5.1817E-13	5.1613E-13	5.2E-13	5.28502E-13
30	4.50586E-13	4.45006E-13	4.4297E-13	4.46E-13	4.55338E-13
35	3.84324E-13	3.78744E-13	3.767E-13	3.8E-13	3.89076E-13
40	3.24964E-13	3.19384E-13	3.1734E-13	3.21E-13	3.29716E-13
45	2.72506E-13	2.66926E-13	2.6489E-13	2.68E-13	2.77258E-13
50	2.2695E-13	2.2137E-13	2.1933E-13	2.23E-13	2.31702E-13
55	1.88296E-13	1.82716E-13	1.8068E-13	1.84E-13	1.93048E-13
60	1.56544E-13	1.50964E-13	1.4892E-13	1.52E-13	1.61296E-13
65	1.31694E-13	1.26114E-13	1.2407E-13	1.28E-13	1.36446E-13
70	1.13746E-13	1.08166E-13	1.0613E-13	1.1E-13	1.18488E-13
75	1.027E-13	9.71203E-14	9.5081E-14	9.85E-14	1.07452E-13
80	9.8556E-14	9.29763E-14	9.0937E-14	9.44E-14	1.03308E-13
85	1.01314E-13	9.57343E-14	9.3695E-14	9.71E-14	1.06066E-13
90	1.10974E-13	1.05394E-13	1.0335E-13	1.07E-13	1.15726E-13
95	1.27536E-13	1.21956E-13	1.1992E-13	1.23E-13	1.32288E-13
100	1.51E-13	1.4542E-13	1.4338E-13	1.47E-13	1.55752E-13

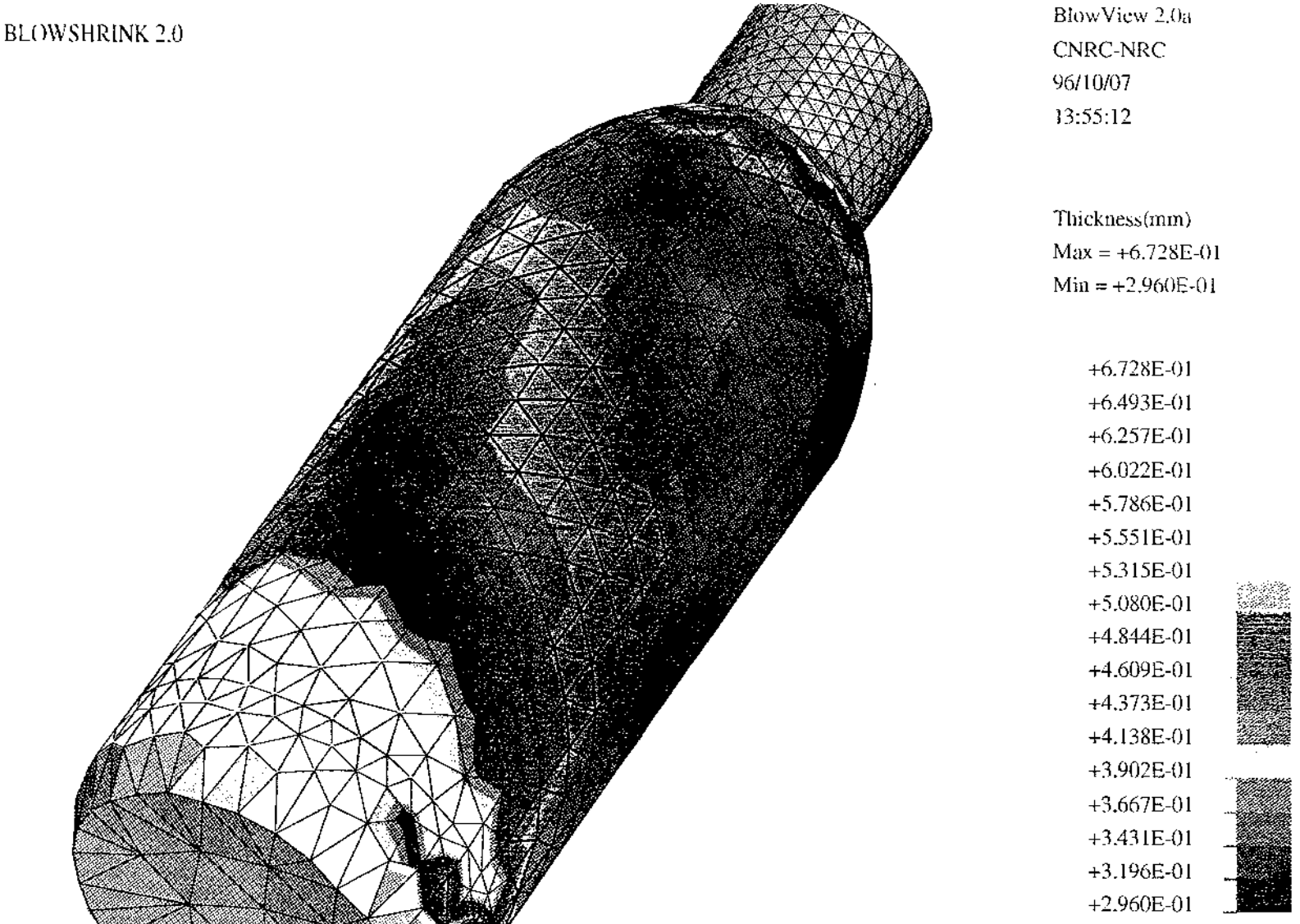

Appendix I : Thickness distribution of blow moulded bottle